

© 2020. T. Zdeb.

This is an open-access article distributed under the terms of the Creative Commons Attribution-NonCommercial-NoDerivatives License (CC BY-NC-ND 4.0, <https://creativecommons.org/licenses/by-nc-nd/4.0/>), which permits use, distribution, and reproduction in any medium, provided that the Article is properly cited, the use is non-commercial, and no modifications or adaptations are made.



INTERFACIAL TRANSITION ZONE IN REACTIVE POWDER CONCRETES (RPC) CURED UNDER VARIOUS HYDROTHERMAL CONDITIONS

T. ZDEB¹

Reactive powder concrete (RPC), due to its characteristic composition with reduced water quantity, often below a stoichiometric ratio, the addition of pozzolana usually close to or above 20% of the weight of cement and a significantly reduced inclusion rate compared to normal or high performance concrete, has a different nature of the interfacial transition zone between the micro aggregate grains and the binder matrix. Due to the significant influence of RPC curing conditions on the morphology of the interfacial transition zone, the analysis included composites cured in water of $T_{\max}=20^{\circ}\text{C}$, subject to low-pressure steam curing $T_{\max}=90^{\circ}\text{C}$ and autoclaved at $T_{\max}=250^{\circ}\text{C}$. The paper presents a qualitative assessment of the interfacial transition zone in reactive powder concretes with the use of a scanning microscope with the use of linear EDS and quantitative analysis by means of stereological analysis of the image obtained with the use of a BSE detector. The results of the study unequivocally confirm the lack of portlandite crystallisation at the phase interface and the different phase composition in the interfacial transition zone in relation to the mean mass composition.

Keywords: Interfacial Transition Zone, Reactive Powder Concrete RPC, Steaming, Autoclaving

¹ Ph.D., Eng., Cracow University of Technology, Faculty of Civil Engineering, Ul. Warszawska 24, 31-155 Cracow, Poland, e-mail: tomasz.zdeb@pk.edu.pl

1. INTRODUCTION

The evolution of the description of the interfacial transition zone in cement composites was traced by Kurdowski [1], whereby he characterised its generally accepted models, including those by De Rooij et al. [2], Roy and Landgtou [3], Barnes et al. [4], differentiated in terms of successive zones and their phase composition. The development of the methodology of research of the interfacial transition zone, in turn, enables an ever more precise description of the properties and structure of this sensitive part of cement granular composites. The most common methods applied are optical and scanning microscopy [5–9] together with stereological image analysis, EDS analysis [10–12], XRD analysis [13–15], as well as nanoindentation [16, 17].

In the case of traditional cement composites, the interfacial transition zone (ITZ) plays an important role in the shaping of their mechanical properties due to the area where crack initiation in loaded material most frequently occurs. Therefore, one of the basic ideas of selecting the composition of RPC composites is homogenisation of the texture of the composite having direct connection with homogenisation of actual stresses in the loaded material. Godycki-Ćwirko in [18] explains how intensively the value of actual stresses is affected by: inclusion rate, mutual distance between its grains and difference in inclusion deformability in relation to the matrix. While it is impossible to change the mechanical properties of the applied inclusion (in the case of RPC, most often – β -quartz grains), in the case of the binder matrix, consisting mainly of calcium silicate hydrates [19], some researchers claim that it may be slightly modified. The studies published in [20] indicate a slight upward trend in the modulus of elasticity of the C-S-H phase following a decrease in the Ca/Si ratio. On the other hand, according to the authors of [21] studies conducted with the nanoindentation method indicate that the C-S-H phase produced with silica fume in the amount from 0 to 20% of cement weight does not exhibit any changes in deformation properties. The measured modulus of elasticity ranged from 18.2 to 18.5 GPa. The slight changes of deformation properties described in [21] and [20] are not significant from the point of view of the modulus of elasticity of quartz inclusions, which is over 43 GPa (also determined by the nanoindentation method). The remaining factors affecting the homogeneity of the actual stresses, according to the basic assumptions of RPC design [22], are implemented by limiting the inclusion volume to approximately 40%, which results in increasing the mutual distance between the grains and ultimately in decreasing the maximum grain size below 1 mm. However, despite the use of the aforementioned material solutions, although in a

significantly reduced form, the problem of local stress increase in the interfacial transition zone between the inclusion grain and the matrix remains.

An attempt to characterise the interfacial transition zone between the binder matrix and the micro quartz aggregate in reactive powder concretes maturing in various hydrothermal conditions is described below. These conditions influence the reactivity of individual components of the composite and thus the phase composition of the interfacial transition zone. Materials cured in natural conditions, subjected to low-pressure steam curing and autoclaving were analysed.

2. MATERIALS AND TESTING METHODOLOGY

RPC composite mixes were made of the following components: Portland cement CEM I 52.5 R, silica fume, ground quartz 0/0.2 mm, quartz sand 0/0.5 mm, polycarboxylate superplasticiser and mixing water in the amount of $w/b=0.20$. The characteristics of individual components are presented in Tables 1 – 3.

Table 1. Chemical and phase composition as well as basic characteristics of CEM I 52.5 R

<i>Properties</i>	
Initial setting time [min]	130
Final setting time [min]	220
Specific surface area [cm ² /g]	4100
Compressive strength after 2 days [MPa]	34.5
Compressive strength after 28 days [MPa]	70.8
<i>Chemical composition [wt. %]</i>	
CaO – 65.6; SiO ₂ – 23.0; Al ₂ O ₃ – 4.4; Fe ₂ O ₃ – 2.1; SO ₃ – 3.3; MgO – 1.0; Na ₂ O _e – 0.5; Cl ⁻ – 0.009 LOI – 1.4	
<i>Phase composition [wt. %]</i>	
C ₃ S – 59.1; C ₂ S – 18.0; C ₃ A – 8.1; C ₄ AF – 6.4	

The fraction of individual components in the RPC composite was determined in such a way as to obtain maximum packing density of dry components and an appropriate consistency of the mix. Obtaining the maximum packing density of dry components was based on the experiments of Funk and Dinger [23], who proposed a formulation for a function describing the optimal grain size distribution, which can also be applied when designing the composition of highly fine-grained materials. Knowing the precise grain size distribution of the individual components of the micro aggregate, it is possible to determine the optimum proportions on the basis of the aforementioned

curve. In case of conducted tests, the amount of quartz dust in relation to quartz sand should be 30/70. When using silica fume in the amount of 20% of cement mass, the most advantageous volume fraction of micro aggregate to the volume of the binder matrix was 40/60. The precise composition of the RPC mix is presented in Table 4.

Table 2. Parameters of particle size distribution and chemical composition of ground quartz and quartz sand

<i>Properties</i>	<i>Ground quartz</i>	<i>Quartz sand</i>
D_{max} [μm]	200	500
D_{50} [μm]	16	110
Specific surface BET [m^2/g]	0.8	0.04
Density [g/cm^3]	2.65	
Polymorphic modification	β -quartz	
SiO_2 [%]	99.0	98.5
Al_2O_3 [%]	0.3	0.8
Fe_2O_3 [%]	0.05	0.03

Table 3. Properties and chemical composition of silica fume

<i>Properties</i>	
Specific surface area BET [m^2/g]	22.4
Density [g/cm^3]	2.23
<i>Chemical composition [wt. %]</i>	
SiO_2 – 94.06; Al_2O_3 – 0.74; Fe_2O_3 – 0.78; CaO – 0.06; MgO – 0.49; Na_2O_e – 1.43; SO_3 – 0.63; LOI – 0.74	

Table 4. Mix proportion of the RPC

<i>Component</i>	<i>Mass fraction [kg/m^3]</i>
Cement CEM I 52.5 R	903
Silica fume	181
Ground quartz 0/0.20 mm	312
Quartz sand 0/0.50 mm	729
Water	217
Superplasticiser	19.4

After mixing the components, a mix was obtained with a flow of 25 cm, measured according to the procedure described in [24]. Then, 3 specimens of 40x40x160 mm were formed and cured under the

following three conditions. The values of individual hydrothermal treatment parameters were adopted on the basis of the results of the studies described in [25].

- Natural curing in water at a temperature of 20°C for 28 days.
- Low-pressure steam curing in hydrothermal conditions (initial curing – 6h; temperature increase from 20 to 90°C – 3h; isothermal heating – 12h; cooling down to 20°C – 3h).
- Curing in hydrothermal conditions with autoclaving (initial curing – 24h; temperature increase from 20 to 250°C – 12h; isothermal heating – 12h; cooling down to 20°C – 12h).

The RPC composites obtained in this way were subjected to strength tests after 28 days of curing in water or in the case of hydrothermally treated after cooling to ambient temperature. The average tensile strength at bending was determined on the basis of 3 beams, while the average compressive strength on the basis of 6 cubes cut after bending. In the case of curing in water compressive and tensile strength was equal to 180 and 11 MPa, respectively, while 190 and 14 MPa after low-pressure steaming, and 250 and 19 MPa after autoclaving. Subsequently, after 28 days all specimens with a surface area of 20x20 mm were cut from the bars remains for observation in a scanning microscope, from which microsections were prepared. The observations were made using a Zeiss EVO10 M scanning microscope equipped with an EDS detector. The specimens prepared as described were used for qualitative and quantitative testing of the interfacial transition zone around the grains of quartz sand. Qualitative tests were carried out on the surface of three randomly selected grains of quartz sand, each time carrying out five EDS linear analyses directed perpendicularly to the surface of the grain (see Fig. 1).

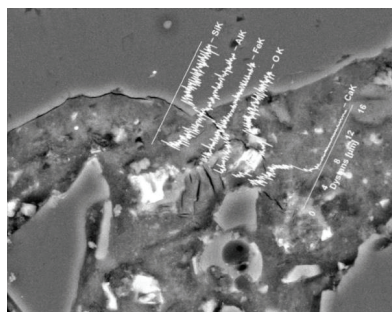


Fig. 1. Example results of linear EDS analysis of the interfacial transition zone in RPC – curing in water

In order to quantitatively describe the phases occurring around micro aggregate grains in RPC composites, stereological analysis was applied using the Cavalieri principle, according to which the volume fraction of the i -th phase of the composite V_V , its fraction in the cross-section surface area

A_A and the length of the section per this phase in relation to the length of the section representative of the entire composite L_L can be expressed with the same number.

$$V_V = A_A = L_L \quad (5)$$

The test procedure was adopted analogous to those described by Diamond in [5, 9]. It is based on a stereological analysis of the image reduced to grayscale, in the area removed from the edge of the aggregate grain by 10, 20, 30, 40 and 50 μm , respectively. The histogram of the image obtained in this manner, describing the number of pixels assigned to a specific grayscale value on a scale from 0 to 255, is the basis for quantifying the phase fraction in the examined area. Each time, this scale is divided into four parts, from the brightest to the darkest, to assign the phases, respectively: relics of cement grains, C-S-H, quartz grains and pores. To facilitate determining the number of pixels assigned to a specific phase, once the grayscale range was determined, the image was transposed to binary mode (see Fig. 2). Photos were taken at 1000x magnification at a resolution of 2024x1886 pixels. The number of measurements, i.e. the size of the analysed area was selected so that the relative standard measurement error would not exceed 2% [9]. As a reference analysis, analogous studies of the entire observed area of the material structure were conducted, which enabled the verification of differences in the quantitative fractions of particular phases around the micro aggregate grains (ITZ) in relation to their fraction in the "mass" of the entire composite.

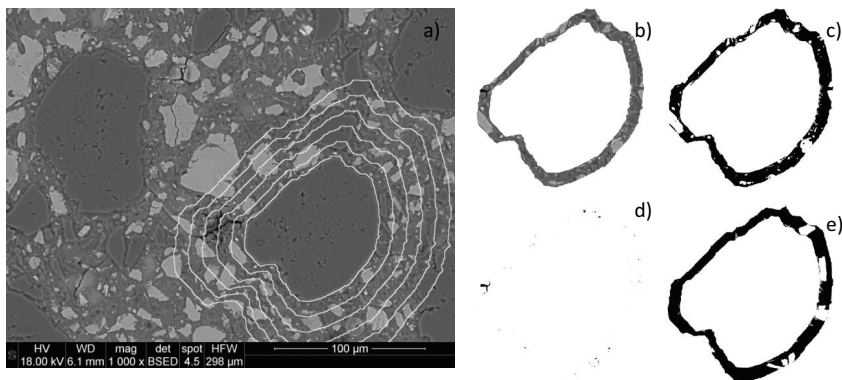


Fig. 2. Quantitative phase analysis around RPC micrograins – schematic representation;
(a) areas subjected to stereological analysis in the range of 0 to 50 μm ; (b) image of a section of the analysed image; (c) binary image of the relics of cement grains; (d) binary image of pores;
(e) binary image of quartz grains

3. RESEARCH RESULTS AND DISCUSSION

The completed EDS linear analyses (see Fig. 1) enabled the determination of the ratio of the number of Ca, Si, Al and Fe atoms in the entire adopted line length range and thus for each point on the line with a resolution of approx. every 0.05 μm . On this basis, a cloud of measurement points was created in the Ca/Si – Al+Fe/Ca coordinate system, where additionally the areas of occurrence of phases possibly found in the composite were marked. As you can see from the charts in Fig. 3, in all cases of curing conditions, i.e. in water, during low-pressure steam curing and autoclaving, only the C-S-H phase remains in direct contact in the interfacial transition zone. In no case has a Ca/Si ratio been observed which could indicate crystallisation of CH or AFm in the analysed zone. The results of these observations are consistent with the results of XRD studies published in [26], where a trace fraction of calcium hydroxide was confirmed in this type of composites. As can be seen in Fig. 3a and 3b, in the case of curing in water and during steam curing, inclusions of unreacted cement grains often appear in the vicinity of quartz inclusions. However, the increase in cement hydration during autoclaving, which was also verified by the studies described in [27], can also be noted in the observations of the contact zone. The number of points assigned to the area of occurrence of alite grains is significantly lower. What is also important, in the area of the C-S-H phase, materials subjected to autoclaving show a reduced Ca/Si ratio (see Fig. 3c). A clear increase in the solubility of silica in the form of not only silica fume but, as can be assumed from the numerous pits on the surface of the micro aggregate grains, also the silica constituting this inclusion, is evident here (see Fig. 5b).

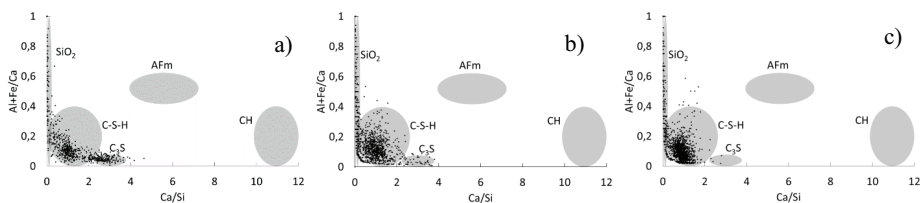


Fig. 3. The relation of the ratio of the number of Ca/Si atoms to Al+Fe/Ca atoms in the interfacial transition zone observed in RPC cured a) in water, b) in low-pressure steam curing conditions, c) in an autoclave

Fig. 4 presents the variability of the fraction of the primary phases in RPC cured in different analysed conditions, depending on the distance from the surface of aggregate grains.

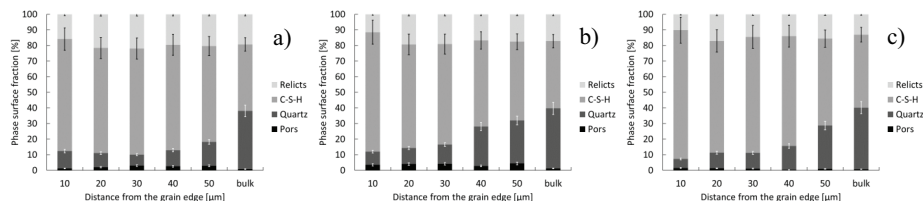


Fig. 4. Change in the fraction of RPC composite phases with increasing distance from the edge of the quartz inclusion in relation to the total volume of the material a) curing in water, b) low pressure steam curing, c) autoclaving

In general, it can be stated that the conducted stereological analysis of the specimens satisfactorily describes the actual composition of the composite. The volume fraction of quartz grains V_Q in the observed areas in relation to the designed RPC composition differs only from 0.5 to 2.7% (actual composition: $V_Q=40\%$; stereological analysis: $V_Q=37.3 - 39.5\%$, depending on curing conditions). On the other hand, the degree of cement hydration in RPC composite can be estimated on the basis of the analysis of the volume fraction of the relics of cement grains. As a starting point, on the basis of the composition presented in Table 4, the volume fraction of cement grains before the start of the hydration process should be 29.1%. The actual fractions of relics in the case of curing in water, low-pressure steam curing and autoclaving are, respectively: 19.3, 17.2 and 13.1%. Therefore, as can be easily calculated, the degrees of the hydration of cement α in the three cases of curing conditions under consideration are: 33.7, 40.9 and 54.9%. As for the verification of the porosity of the composite by the method described above, the darkest areas qualified as free space of the composite were observed mainly as micro-cracks occurring in the matrix of the composite, i.e. the C-S-H phase or around the edges of quartz grains (mainly in composites cured in water and subjected to low-pressure hydrothermal treatment – see Fig. 2). Therefore, the values obtained should not be related to RPC porosity described by other methods, e.g. helium pycnometer or mercury porosimetry.

The analysis of conducted stereological studies indicates that regardless of the method applied for composite curing, the tendency of occurrence of particular phases in the environment of micro aggregate grains is similar. In the immediate vicinity of the micro aggregate grain (0 – 10 μm), the C-S-H phase is predominant. Its fraction is significantly higher in relation to the amount present in the mass of material by approximately 70% and constitutes on average 77% of the analysed surface. The increase in the proportion of calcium silicate hydrates takes place at the expense of quartz grains, but also unhydrated cement grains and is differentiated in relation to the curing conditions of the composite. While in the case of curing in water and low pressure steam curing the values are similar

and amount to 72% and 76%, respectively, in the case of autoclaving, the effect of an increase in the degree of cement hydration is notable, since the proportion of the C-S-H phase around the quartz grains is above 82%. The number of relics of cement grains decreases with the increase in the composite curing temperatures, both in the immediate vicinity of inclusion and in the entire volume of the material. Comparing the surface of relics in the space between 0 and 10 μm to the surface of this inclusion in relation to the entire material, this value increases from approximately 3 to 5% depending on the curing conditions. Therefore, as in the case of ordinary cement composites, RPC materials show a similar trend of limited relics of cement grains around the aggregate. However, due to a very small amount of water ($w/b=0.20$) the effect of cement hydration increase attributable to the local increase in the water-binder ratio should not be expected here, but, as confirmed by a significantly limited number of quartz grains, the wall effect can be indicated as the main reason for the different phase composition in the interfacial transition zone with respect to the entire composite. The sum of the relative surface areas assigned to unhydrated cement grains and quartz grains increases with the distance from the edge of inclusion. Initially, at a distance of up to 10 μm from the edge of the inclusion, it amounts to 16% in the case of autoclaving and 27% in the case of water curing, maintaining an upward trend with increasing the distance from the analysed edge of the aggregate. At a distance of 50 μm , the sum of the surface areas of both inclusions in all cases of ripening conditions is approximately 40%, on average. However, it still does not reach the representative value for the entire material, which is around 60%.

Additional microscopic observations have shown that RPC composites subjected to autoclaving have unique properties. Their curing at high temperature and pressure conditions (T_{max} up to 250°C at water vapour pressure $P_{\text{H}_2\text{O}}=3.9$ MPa) leads to significant changes in the microstructure, involving crystallisation of calcium silicate hydrates (see Fig. 5).

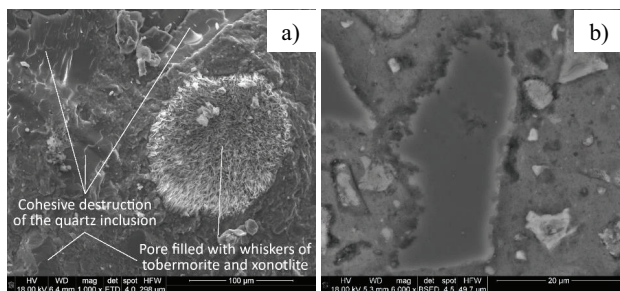


Fig. 5. (a) microphotography of a fracture in the RPC subjected to autoclaving, (b) characteristic pitting on the surface of the quartz inclusion in the RPC subjected to autoclaving

According to the literature, these crystals mainly include whiskers of tobermorite and xonotlite [28–31]. Moreover, the texture of the autoclaved composite is characterised by pitting on the surface of quartz grains, which indicates the topochemical reaction of the binder matrix with this essentially inert inclusion (Fig. 5b). This reaction causes an increase in the mutual adhesion of the described phases to such an extent that practically no adhesion damage is observed at the fractures (Fig. 5a). This is also reflected in the mechanical properties of the composite. In relation to water curing, compressive strength increases by almost 40% and tensile strength at bending even by over 70% when the RPC composition is constant. Detailed results of the mechanical properties of the described composites can be found in the publication [32]. As mentioned above, in the case of curing in water and low-pressure steam curing, numerous micro-cracks can be observed at the phase boundary between quartz grains and generally the C-S-H phase. Their presence in the material subjected to tensile stress may lead to relatively easy propagation. In the case of autoclaved materials, such defects are practically never observed, which at the same time results in a virtually exclusively cohesive character of composite damage.

4. SUMMARY AND CONCLUSIONS

Both literature reports and own research results based on typical RPC composition, indicate no presence of an interfacial transition zone similar to ordinary cement composites. The main reason for this situation can be provided by the composition of RPC composites, in which the amount of mixing water is often limited to below stoichiometric value, while the amount of pozzolana added mainly in the form of silica fume is rarely lower than 20% of cement mass. Furthermore, as EDS linear analysis indicates, the frequently applied curing method in conditions of elevated temperature promotes the solubility of silica, confirmed by a reduction in the Ca/Si ratio, which in turn modifies the phase composition of hydration products in the mass, as well as in the interfacial transition zone.

Based on both EDS linear and stereological analysis of the areas around the grains of quartz sand in tested RPC, it can be stated that the main component in the interfacial transition zone is the amorphous C-S-H phase which, depending on the curing conditions, takes from 72 to 82% of the space up to 10 μm around the quartz sand grains. Moreover, regardless of the curing conditions, no portlandite crystals were observed in the ITZ. Furthermore, limited content of cement grain relics was also observed in all analysed curing conditions. However, in the case of RPC composites, this is not attributable to the locally increased degree of cement hydration, but rather to the wall effect, which

is also confirmed by the distribution of small grains of ground quartz around relatively large grains of quartz sand.

The stereological analysis of the tested RPC microsections is a good method for the quantification of phases occurring in this composites, which was confirmed on the basis of the amount of quartz in the actual composition of the tested RPC in relation to the amount determined by the method in question. The volume fraction of quartz grains in relation to actual composition differs only from 0.5 to 2.7%, depending on the curing conditions. Moreover, curing of the RPC under hydrothermal conditions leads to an increase in the degree of cement hydration by approximately 20 and 60% compared to curing in water, in the case of low-pressure steam curing and autoclaving respectively.

REFERENCES

1. Kurdowski, W.: *Cement and Concrete Chemistry*. Springer Netherlands (2014).
2. De Rooij, M.R., Bijen, J.M., Frens, G.: Introduction of Syneresis in Cement Paste. In: *Second International Conference on the Interfacial Transition Zone in Cementitious Composites*, Rilem proceedings. , Haifa, Isarel (1998).
3. Roy, D.M., Langton, C.A.: Morphology and Microstructure of Cement Paste-Rock Interfacial Regions. In: *7th Int. Congr. Chem. Cem.ICCC*. p. Vol. 3 VII-127. , Paris (1980).
4. Barnes, B.D., Diamond, S., Dolch, W.L.: The contact zone between portland cement paste and glass "aggregate" surfaces. *Cem. Concr. Res.* 8, (1978).
5. Diamond, S., Huang, J.: The ITZ in concrete—a different view based on image analysis and SEM observations. *Cem. Concr. Compos.* 23, 179–188 (2001).
6. Vargas, P., Restrepo-Baena, O., Tobón, J.I.: Microstructural analysis of interfacial transition zone (ITZ) and its impact on the compressive strength of lightweight concretes. *Constr. Build. Mater.* 137, 381–389 (2017). <https://doi.org/10.1016/j.conbuildmat.2017.01.101>.
7. Xie, Y., Corr, D.J., Jin, F., Zhou, H., Shah, S.P.: Experimental study of the interfacial transition zone (ITZ) of model rock-filled concrete (RFC). *Cem. Concr. Compos.* 55, 223–231 (2015). <https://doi.org/10.1016/j.cemconcomp.2014.09.002>.
8. Elsharief, A., Cohen, M.D., Olek, J.: Influence of aggregate size, water cement ratio and age on the microstructure of the interfacial transition zone. *Cem. Concr. Res.* 33, 1837–1849 (2003). [https://doi.org/10.1016/S0008-8846\(03\)00205-9](https://doi.org/10.1016/S0008-8846(03)00205-9).
9. Diamond, S.: Considerations in image analysis as applied to investigations of the ITZ in concrete. *Cem. Concr. Compos.* 23, 171–178 (2001). [https://doi.org/10.1016/S0958-9465\(00\)00085-8](https://doi.org/10.1016/S0958-9465(00)00085-8)
10. Cwirzen, a.: The effect of the heat-treatment regime on the properties of reactive powder concrete. *Adv. Cem. Res.* 19, 25–33 (2007). <https://doi.org/10.1680/adcr.2007.19.1.25>.
11. Erdem, S., Dawson, A.R., Thom, N.H.: Influence of the micro- and nanoscale local mechanical properties of the interfacial transition zone on impact behavior of concrete made with different aggregates. *Cem. Concr. Res.* 42, 447–458 (2012). <https://doi.org/10.1016/j.cemconres.2011.11.015>.
12. Trägårdh, J.: Microstructural features and related properties of self compacting concrete. In: *Proceedings of the First International RILEM Symposium on Self Compacting Concrete* (1999).
13. Yue, L., Shuguang, H.: The microstructure of the interfacial transition zone between steel and cement paste. *Cem. Concr. Res.* 31, 385–388 (2001). [https://doi.org/10.1016/S0008-8846\(01\)00452-5](https://doi.org/10.1016/S0008-8846(01)00452-5).
14. Grandet, J., Ollivier, J.P.: New method for the study of cement - aggregate interfaces. In: *7th Int. Congr. Chem. Cem.* pp. 85–89. , Rio de Janeiro (1986).
15. Zhang, Z., Zhang, B., Yan, P.: Comparative study of effect of raw and densified silica fume in the paste, mortar and concrete. *Constr. Build. Mater.* 105, 82–93 (2016). <https://doi.org/10.1016/j.conbuildmat.2015.12.045>.
16. Allison, P.G., Moser, R.D., Chandler, M.Q., Rushing, T.S., Williams, B.A., Cummins, T.K.: Nanomechanical structure-property relations of dynamically loaded reactive powder concrete. *WIT Trans. Eng. Sci.* 72, 287–298 (2011). <https://doi.org/10.2495/MC110251>.

17. Rossignolo, J.A., Rodrigues, M.S., Frias, M., Santos, S.F., Junior, H.S.: Improved interfacial transition zone between aggregate-cementitious matrix by addition sugarcane industrial ash. *Cem. Concr. Compos.* 80, 157–167 (2017). <https://doi.org/10.1016/j.cemconcomp.2017.03.011>.
18. Godycki Ćwirko, T.: *Mechanika betonu*. Arkady, Warszawa (1982).
19. Korpa, A., Kowald, T., Trettin, R.: Phase development in normal and ultra high performance cementitious systems by quantitative X-ray analysis and thermoanalytical methods. *Cem. Concr. Res.* 39, 69–76 (2009). <https://doi.org/10.1016/j.cemconres.2008.11.003>.
20. Hu, C., Li, Z.: Property investigation of individual phases in cementitious composites containing silica fume and fly ash. *Cem. Concr. Compos.* 57, 17–26 (2015).
21. Garcia, D.C.S., Soares, M.M.N. de S., Bezerra, A.C. da S., Aguilar, M.T.P., Figueiredo, R.B.: Microstructure and hardness of cement pastes with mineral admixture. *Rev. Mater.* 22, (2017). <https://doi.org/10.1590/S1517-707620170002.0145>.
22. Richard, P., Cheyrezy, M.: Composition of reactive powder concretes. *Cem. Concr. Res.* 25, 1501–1511 (1995).
23. Funk, J.E., Dinger, D.R.: Introduction to Predictive Process Control. In: *Predictive Process Control of Crowded Particulate Suspensions*. pp. 1–16 (1994).
24. EN 1015-3: Methods of test for mortar for masonry. Determination of consistence of fresh mortar (by flow table). (1999).
25. Zdeb, T.: An analysis of the steam curing and autoclaving process parameters for reactive powder concretes. *Constr. Build. Mater.* 131, 758–766 (2016). <https://doi.org/10.1016/j.conbuildmat.2016.11.026>.
26. Zdeb, T.: The impact of composition and technology on selected properties of reactive powder concretes., (2009).
27. Zdeb, T.: Autogenous Healing Effect of Ultra-High Performance Cementitious Composites. *J. Adv. Concr. Technol.* 16, 549–562 (2018). <https://doi.org/10.3151/jact.16.549>.
28. Feylessoufi, A., Crespin, M., Dion, P., Bergaya, F., Van Damme, H., Richard, P.: Controlled Rate Thermal Treatment of Reactive Powder Concretes. *Adv. Cem. Based Mater.* 6, 21–27 (1997).
29. Philippot, S., Masse, S., Zanni, H., Nieto, P., Maret, V., Cheyrezy, M., Physique, L. De, Mccanique, D., Cnrs, U.R.: ²⁹Si NMR study of hydratation and pozzolanic reactions in reactive powder concrete (RPC). *Magn. Reson. Imaging.* 14, 891–893 (1996).
30. Lehmann, C., Fontana, P., Müller, U.: Evolution of Phases and Micro Structure in Hydrothermally Cured Ultra-High Performance Concrete (UHPC). *Nanotechnol. Constr.* 3 - Proc. NICOM3 . 287–294 (2009).
31. Müller, U., Kuhne, H., Fontana, P., Meng, B., Nemecek, J.: Micro texture and mechanical properties of heat treated and autoclaved Ultra High Performance Concrete (UHPC). In: Fehling, E., Schmidt, M., and Sturwald, S. (eds.) *Second International Symposium on Ultra High Performance Concrete*. pp. 211–220. , Kassel, Germany (2008).
32. Zdeb, T.: Effect of vacuum mixing and curing conditions on mechanical properties and porosity of reactive powder concretes. *Constr. Build. Mater.* 209, 326–339 (2019).

LIST OF FIGURES AND TABLES:

Fig. 1. Example results of linear EDS analysis of the interfacial transition zone in RPC – curing in water

Rys. 1. Przykładowe wyniki analizy liniowej EDS strefy przejściowej w BPR – dojrzewanie w wodzie

Fig. 2. Quantitative phase analysis around RPC micrograins – schematic representation; (a) areas subjected to stereological analysis in the range of 0 to 50 μm ; (b) image of a section of the analysed image; (c) binary image of the relics of cement grains; (d) binary image of pores; (e) binary image of quartz grains

Rys. 2. Schemat ilościowej analizy fazowej wokół ziaren mikrokruszywa BPR; a) obszary poddane analizie stereologicznej w zakresie od 0 do 50 μm ; b) obraz wycinka analizowanego obrazu; c) obraz binarny relików ziaren cementu; d) obraz binarny porów; e) obraz binarny ziaren kwarcowych

Fig. 3. The relation of the ratio of the number of Ca/Si atoms to Al+Fe/Ca atoms in the interfacial transition zone observed in RPC cured a) in water, b) in low-pressure steam curing conditions, c) in an autoclave

Rys. 3. Zależność proporcji liczby atomów Ca/Si względem Al+Fe/Ca w strefie przejściowej obserwowanej w BPR dojrzewającym a) w wodzie, b) w warunkach niskoprężnego naparzeni, c) w autoklawie

Fig. 4. Change in the fraction of RPC composite phases with increasing distance from the edge of the quartz inclusion in relation to the total volume of the material a) curing in water, b) low pressure steam curing, c) autoclaving

Rys. 4. Zmiana udziału faz kompozytu BPR wraz ze zwiększającym się dystansem od krawędzi inkluzji kwarcowej względem całkowitej objętości materiału a) dojrzewanie w wodzie, b) niskoprężne naparzenie, c) autoklawizacja

Fig. 5. (a) microphotography of a fracture in the RPC subjected to autoclaving, (b) characteristic pitting on the surface of the quartz inclusion in the RPC subjected to autoclaving

Rys. 5. (a) mikrofotografia przełamu BPR poddanego procesowi autoklawizacji, (b) charakterystyczne wżery na powierzchni kwarcowej inkluzji w BPR poddanego procesowi autoklawizacji

Tab. 1. Chemical and phase composition as well as basic characteristics of CEM I 52.5 R

Tab. 1. Skład chemiczny i fazowy oraz podstawowe właściwości CEM I 52.5 R

Tab. 2. Parameters of particle size distribution and chemical composition of ground quartz and quartz sand

Tab. 2. Parametry uziarnienia oraz skład chemiczny piasku i mączki kwarcowej

Tab. 3. Properties and chemical composition of silica fume

Tab. 3. Właściwości i skład chemiczny pyłu krzemionkowego

Tab. 4. Mix proportion of the RPC

Tab. 4. Skład mieszanki BPR

STREFA PRZEJŚCIOWA W BETONACH Z PROSZKÓW REAKTYWNYCH BPR DOJRZEWAJĄCYCH W RÓŻNYCH WARUNKACH HYDROTHERMALNYCH

Słowa kluczowe: strefa przejściowa, beton z proszków reaktywnych BPR, niskoprężne naparzenie, autoklawizacja

STRESZCZENIE:

Wstęp

Ewolucję opisu strefy przejściowej w kompozytach cementowych prześledził Kurdowski w publikacji „Chemia Cementu i Betonu”, gdzie scharakteryzował jej ogólnie przyjęte modele zróżnicowane pod względem występujących kolejno po sobie stref, jak i pod względem ich składu fazowego. Ponadto rozwój metodyki badań strefy przejściowej pozwala obecnie coraz ściślej opisywać właściwości oraz budowę tej newralgicznej części cementowych kompozytów ziarnistych. Stosuje się tutaj najczęściej metodę mikroskopii zarówno optycznej jak i skaningowej wraz ze stereologiczną analizą obrazu, analizę EDS, XRD, a także w celu rozpoznania różnic we właściwościach mechanicznych względem kruszywa i matrycy stosuje się badania metodą nanoindentacji.

W przypadku tradycyjnych kompozytów cementowych strefa przejściowa odgrywa ważną rolę w kształtowaniu ich cech mechanicznych ze względu na obszar, w którym najczęściej dochodzi do zainicjowania rys w obciążonym materiale. Z tego względu, jedną z podstawowych idei komponowania składu kompozytów BPR jest homogenizacja tekstury kompozytu, mająca bezpośredni związek z ujednorodnieniem rzeczywistych naprężeń panujących w obciążonym materiale. Godycki-Ćwirko tłumaczy, jak intensywnie na wartość naprężeń rzeczywistych wpływa: wielkość inkluzji, wzajemna odległość pomiędzy jej ziarnami oraz różnica w odkształcalności inkluzji względem matrycy. Ponadto, na charakter strefy przejściowej mają także warunki dojrzewania kompozytu. Z tego powodu w części badawczej niniejszego artykułu scharakteryzowano strefę przejściową pomiędzy matrycą spoiwową i mikrokruszywem kwarcowym w betonach z proszków reaktywnych dojrzewających w zróżnicowanych warunkach hydrotermalnych tj. w wodzie, poddane niskoprężnemu naparzeniu w temperaturze 90°C oraz autoklawizacji w temperaturze 250°C. Warunki te wpływają na reaktywność poszczególnych składników kompozytu i tym samym na skład fazowy strefy przejściowej.

Metodyka badań i materiały

W badaniach wykorzystano standardowy skład mieszanek betonów z proszków reaktywnych, które po dojrzewaniu w wyżej wymienionych warunkach hydrotermalnych zostały poddane obserwacjom mikroskopowym SEM wraz z analizą EDS. Badania jakościowe zostały zrealizowane na powierzchni trzech losowo wybranych ziaren piasku kwarcowego, każdorazowo realizując pięć analiz liniowych EDS ukierunkowanych prostopadle do powierzchni ziarna. Pozwoliły one na wyznaczenie proporcji liczby atomów pierwiastków Ca, Si, Al i Fe w całym przyjętym zakresie długości linii i tym samym w każdym jej punkcie z rozdzielczością około co 0,05 μm . Na tej podstawie naniesiono chmurę punktów pomiarowych w układzie współrzędnych Ca/Si – Al+Fe/Ca, gdzie zaznaczono także obszary występowania możliwych w kompozycie faz tj. C-S-H, CH, C₃S, AFm.

W celu ilościowego opisu faz występujących wokół ziaren mikrokruszywa w kompozytach BPR wykorzystano analizę stereologiczną stosując zasadę Cavalieriego, według której udział objętościowy i-tej fazy kompozytu V_V , jej udział na powierzchni przekroju A_A oraz długość odcinka przypadającego na tę fazę względem długości odcinka reprezentatywnego dla całego kompozytu L_L , można wyrazić tą samą liczbą. Procedurę badań przyjęto analogicznie do opisanych przez Diamonda, która opiera się ona na stereologicznej analizie obrazu zredukowanego do skali szarości, w obszarze oddalonym od krawędzi ziarna kruszywa o kolejno 10, 20, 30, 40 i 50 μm . Histogram uzyskanego w ten sposób obrazu, opisujący liczbę pikseli przypisanych do konkretnej wartości odcienia szarości w skali od 0 do 255, stanowi podstawę ilościowego określenia udziału faz w badanym obszarze.

Najważniejsze wyniki badań i wnioski

Zarówno doniesienia literaturowe jak i uzyskane wyniki badań wskazują na brak obecności strefy przejściowej analogicznej do zwykłych kompozytów cementowych. Główną przyczyną zaistniałej sytuacji można doszukiwać się w składzie kompozytów BPR, w których ilość wody zarobowej często ograniczona jest do wartości poniżej ilości stechiometrycznej, natomiast udział dodatku pucolanowego dodawanego głównie w postaci pyłu krzemionkowego rzadko jest niższy niż 20 % m.c. Ponadto, wyniki analizy liniowej EDS wskazują, że często stosowane dojrzewanie BPR w podwyższonej temperaturze zwiększa rozpuszczalność zawartej w nich krzemionki, co potwierdza obniżona wartość stosunku Ca/Si w badanych obszarach. W istocie wpływa to na skład fazowy produktów hydratacji w masie kompozytów jak i w strefie przejściowej.

Na podstawie liniowej analizy EDS oraz stereologicznej analizy obrazu obszarów wokół ziaren piasku kwarcowego w badanych BPR, można stwierdzić, że głównym składnikiem strefy przejściowej jest amorficzna faza C-S-H, która zajmuje w zależności od warunków dojrzewania od 72 do 82% przestrzeni w otoczeniu do 10 μm od powierzchni ziaren piasku kwarcowego. Ponadto, niezależnie od zastosowanych warunków dojrzewania, nie zaobserwowano śladów krystalizacji portlandytu w strefie przejściowej. Co więcej, we wszystkich przypadkach analizowanych warunków dojrzewania odnotowano ograniczoną zawartość relików ziaren cementowych. Jednak w przypadku kompozytów BPR nie wynika to ze zwiększonego lokalnie stopnia hydratacji cementu, lecz raczej z efektu ściany, co potwierdza także sposób rozmieszczenia drobnych ziaren mączki kwarcowej wokół stosunkowo dużych ziaren piasku kwarcowego.

Zastosowana stereologiczna analiza obrazu zglądów BPR stanowi dobrą metodę ilościowej oceny ich składu fazowego, co zostało potwierdzone przez porównanie udziału kwarcu w zaprojektowanym składzie kompozytu w odniesieniu do

wskazań opisywanej metody. Udział objętościowy ziaren kwarcowych oznaczony metodą analizy obrazu względem rzeczywistego składu różnicował się zaledwie od 0,5 do 2,7%, w zależności od warunków dojrzewania. Ponadto, dojrzewanie kompozytów BPR w warunkach hydrotermalnych prowadzi do wzrostu stopnia hydratacji cementu względem dojrzewania w wodzie o około 20 i 60 %, odpowiednio w przypadku stosowania niskoprężnego naporzenia i autoklawizacji.

Received: 17.02.2020. Revised: 09.09.2020